# Monte Carlo Analysis of the Small-Signal Response of Charge Carriers

H. Kosina, M. Nedjalkov, and S. Selberherr

Institute for Microelectronics, TU-Vienna,
Gusshausstrasse 27-29/E360, A-1040 Wien, Austria
kosina@iue.tuwien.ac.at

**Abstract.** A Monte Carlo method for calculation of the small signal response of charge carriers in semiconductors is presented. The transient Boltzmann equation is linearized with respect to the electric field and an impulse-like perturbation in the field is assumed. The presented formalism allows the impulse response to be explained as a relaxation process, where two carrier ensembles evolve from different inditial distributions to one and the same steady state. Using different methods to generate the initial distributions gives rise to a variety of Monte Carlo algorithms. Both existing and new algorithms for direct simulation of the impulse response are obtained in a unified way. Additionally, the special case of vanishing electric field is considered. Applications to technologically significant semiconductors are shown. For Gallium Arsenide a resonance effect occurring at low temperatures is discussed.

## 1 Introduction

Understanding the Monte Carlo method as a versatile tool to solve integral equations enables its application to a class of problems which are not accessible by purely physically-based, imitative Monte Carlo methods. One such class, which plays an important role in electrical engineering, is the linearized small signal analysis of nonlinear systems. Whether the linearized system is analyzed in the frequency or time domain is just a matter of convenience since the system responses obtained are linked by the Fourier transform. At present, linear small signal analysis of semiconductor devices by the Monte Carlo method is beyond the state of the art. However, recently progress has been made in performing Monte Carlo small signal analysis of bulk carrier transport [1].

## 2 Basic Equations

Choosing a formulation in the time domain, a small perturbation $\mathbf{E}_1$ is superimposed to a stationary field $\mathbf{E}_s$. The stationary distribution function $f_s$ will thus be perturbed by some small quantity $f_1$.

$$\mathbf{E}(t) = \mathbf{E}_s + \mathbf{E}_1(t) \tag{1}$$

$$f(\mathbf{k}, t) = f_s(\mathbf{k}) + f_1(\mathbf{k}, t) \tag{2}$$

S. Margenov, J. Wasniewski, and P. Yalamov (Eds.): ICLSSC 2001, LNCS 2179, pp. 175–182, 2001.

Inserting this Ansatz into the transient Boltzmann equation and retaining only first order perturbation terms yield a Boltzmann-like equation for $f_1$ which is linear in the perturbation $\mathbf{E}_1$.

$$\frac{\partial f_1(\mathbf{k},t)}{\partial t} + \frac{q}{\hbar}\mathbf{E}_s \cdot \nabla f_1(\mathbf{k},t) = Q[f_1](\mathbf{k},t) - \frac{q}{\hbar}\mathbf{E}_1(t) \cdot \nabla f_s(\mathbf{k}) \tag{3}$$

Compared with the common Boltzmann Equation, 3 has an additional term on the right hand side which contains $f_s$, the solution of the stationary Boltzmann Equation. The integro-differential type of equation, 3, is transformed into an integral form. Assuming an impulse-like excitation $\mathbf{E}_1(t) = \delta(t)\mathbf{E}_{\mathrm{im}}$ results in the following integral equation for the impulse response $f_1$.

$$f_1(\mathbf{k},t) = \int_0^t \mathrm{d}t' \int \mathrm{d}\mathbf{k}' f_1(\mathbf{k}',t') S(\mathbf{k}',\mathbf{K}(t')) \mathrm{e}^{-\int_{t'}^{t} \lambda(\mathbf{K}(y)dy} + G(\mathbf{K}(0)) \mathrm{e}^{-\int_0^t \lambda(\mathbf{K}(y)dy} \tag{4}$$

$$G(\mathbf{k}) = -\frac{q}{\hbar}\mathbf{E}_{\mathrm{im}} \cdot \nabla f_s(\mathbf{k}) \tag{5}$$

The free term of 4 is formally equivalent to the free term of the Boltzmann Equation. The only difference is that $G$ takes on also negative values, and can therefore not be interpreted as an initial distribution. Various treatments of the term $G$ can be devised giving rise to a variety of Monte Carlo algorithms, all of which solve 4. In [2] $G$ is expressed as a difference of two positive functions, $G = G^+ - G^-$, an Ansatz which decomposes 4 into two common Boltzmann Equation for the unknowns $f_1^+$ and $f_1^-$. The initial conditions of these Boltzmann Equations are $f_1^{\pm}(\mathbf{k},0) = G^{\pm}(\mathbf{k}) \geq 0$. In this way the impulse response is understood in terms of the concurrent evolution of two carrier ensembles.

Using different methods to generate the initial distributions of the two ensembles gives rise to a variety of Monte Carlo algorithms. Both existing and new Monte Carlo algorithms are obtained in a unified way, and a transparent, physical interpretation of the algorithms is supported.

## 3 The Monte Carlo Algorithm

In the case that the stationary and the small signal field vectors are collinear, the stationary Boltzmann Equation can be used to express the distribution function gradient as

$$G(\mathbf{k}) = \frac{E_{\mathrm{im}}}{E_s}\left(\lambda(\mathbf{k}) f_s(\mathbf{k}) - \int f_s(\mathbf{k}') S(\mathbf{k}',\mathbf{k}) \mathrm{d}\mathbf{k}'\right), \tag{6}$$

which gives a natural splitting of $G$ into two positive functions. In the following we adopt the notation that terms which are employed in the respective algorithm as a probability density are enclosed in curly brackets.

From (6) we choose the initial distributions as

$$G^{+}(\mathbf{k}) = \frac{E_{\mathrm{im}}}{E_s}\langle\lambda\rangle_s \left\{\frac{\lambda(\mathbf{k})f_s(\mathbf{k})}{\langle\lambda\rangle_s}\right\} \tag{7}$$

$$G^{-}(\mathbf{k}') = \frac{E_{\mathrm{im}}}{E_s}\langle\lambda\rangle_s \int \left\{\frac{\lambda(\mathbf{k})f_s(\mathbf{k})}{\langle\lambda\rangle_s}\right\}\left\{\frac{S(\mathbf{k},\mathbf{k}')}{\lambda(\mathbf{k})}\right\}\mathrm{d}\mathbf{k} \tag{8}$$

where $\langle\lambda\rangle_s = \int f_s(\mathbf{k})\lambda(\mathbf{k})\mathrm{d}\mathbf{k}$ is introduced in the denominators to ensure normalization. $\langle\lambda\rangle_s$ is the inverse of the mean free-flight time, which can be seen immediately when evaluating the average by means of the 'before-scattering' method. The probability density $\lambda f_s/\langle\lambda\rangle_s$ represents the normalized distribution function of the before-scattering states. Consequently, the product of the two densities in (8) represents the normalized distribution function of the after-scattering states. Using the above expression the following algorithm can be formulated.

1) Follow a main trajectory for one free flight, store the before-scattering state in $\mathbf{k}_b$, and realize a scattering event from $\mathbf{k}_b$ to $\mathbf{k}_a$.
2) Start a trajectory $\mathbf{K}^{+}(t)$ from $\mathbf{k}_b$ and another trajectory $\mathbf{K}^{-}(t)$ from $\mathbf{k}_a$.
3) Follow both trajectories for time $T$. At equidistant times $t_i$ add $A(\mathbf{K}^{+}(t_i))$ to a histogram $\nu_i^{+}$ and $A(\mathbf{K}^{-}(t_i))$ to a histogram $\nu_i^{-}$.
4) Continue with the first step until $N$ $\mathbf{k}$-points have been generated.
5) Calculate the time discrete impulse response as $\langle A\rangle_{\mathrm{im}}(t_i) = \frac{E_{\mathrm{im}}\langle\lambda\rangle_s}{NE_s}(\nu_i^{+} - \nu_i^{-})$.

The mean free-flight time must be additionally calculated during the simulation. This algorithm shows in a transparent way the evolution of the P and M ensembles, as well as the generation of the initial states for those ensembles.

## 4 Results and Discussion

The following simulation results are obtained by using the new Monte Carlo algorithm. Typical conditions for electrons in Si are considered as well as a special carrier dynamics feature, the Transit Time Resonance (TTR) effect [3][4] for electrons in GaAs. While Si is simulated at 300K, for GaAs the temperature is reduced to 10K to make the TTR effect clearly visible.

Analytical band models are adopted for both Si and GaAs, accounting for isotropic and non-parabolic conduction band valleys. For Si six equivalent X-valleys and for GaAs a three-valley model are included. The used phonon scattering rates can be found, for example, in [5]. Overlap integrals are neglected, and acoustic deformation potential scattering is assumed elastic.

Fig. 1 and Fig. 2 show the time response of the differential electron energy $\partial\langle\epsilon\rangle_{\mathrm{im}}/\partial E_{\mathrm{im}}$ and the longitudinal differential velocity $\partial\langle v\rangle_{\mathrm{im}}/\partial E_{\mathrm{im}}$ for Si at different field strengths. The response characteristics tend to zero when the two ensembles approach the steady state. The characteristic time associated with the relaxation process depicted Fig. 2, namely the momentum relaxation time, clearly decreases with increasing field. This effect is anticipated since the electron

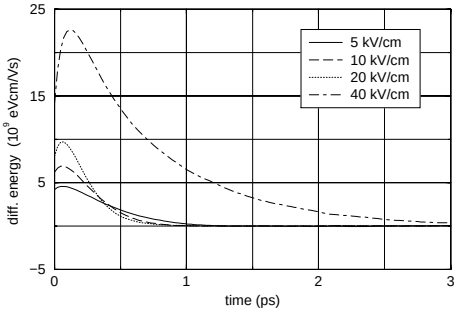


**Fig. 1.** Impulse response of the differential energy.

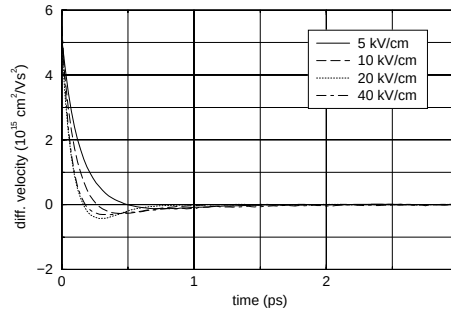


**Fig. 2.** Impulse response of the differential velocity.

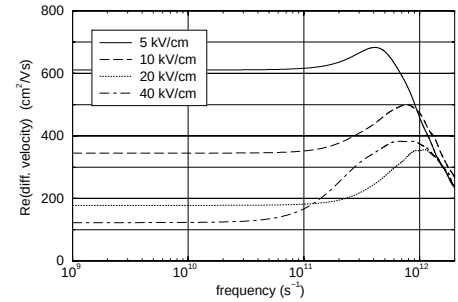


**Fig. 3.** Real part of the differential velocity spectra.

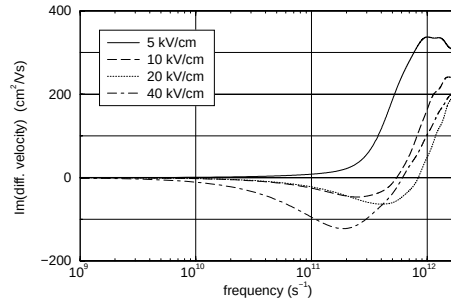


**Fig. 4.** Imaginary part of the differential velocity spectra.

mobility $\mu = e\tau_m/m^*$ is known to show such a field reduction. Generally, within a few ps the steady state is reached by the two ensembles.

Fig. 3 and Fig. 4 show the frequency dependence of the differential velocity obtained by a Fourier transform of the impulse response. The low frequency limits of the imaginary parts tend to zero, while the real parts tend to the corresponding differential mobility values $\partial\langle v\rangle_s/\partial E_s$.

For electrons in $GaAs$ the assumed physical conditions are $T = 10K$ and $E_s = 120V/cm$. In this case all electrons are in the $\Gamma$ valley. In Fig. 5 the differential velocity and differential energy are presented normalized to the respective initial values. The impulse response characteristics reveal a damped oscillation. The pattern is pronounced also in the step response functions on Fig. 6 and Fig. 7 , obtained by time integration of the corresponding impulse response functions.

The pattern appears to be independent of the concrete physical quantity, which leads to the conclusion that a peculiarity of the carrier dynamics is responsible for the behavior. The chosen physical conditions determine a peculiar behavior of the electrons already in the steady-state. Since the acoustical phonon scattering is low (below one scattering for 100ps), the electrons are accelerated by the field until they reach energies above the polar-optical phonon energy

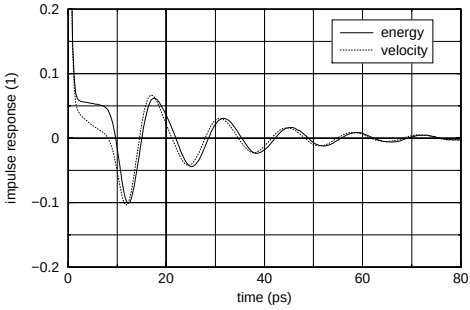


**Fig. 5.** Impulse response of the normalized differential energy and velocity.

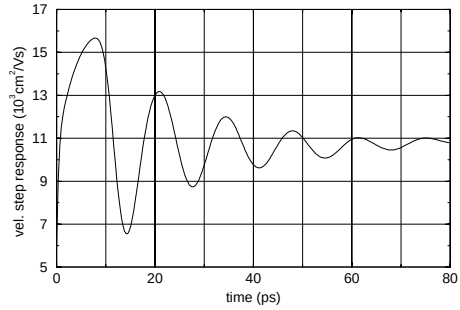


**Fig. 6.** Step response of the differential velocity.

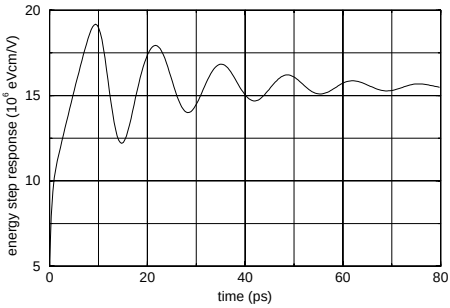


**Fig. 7.** Step response of the differential energy.

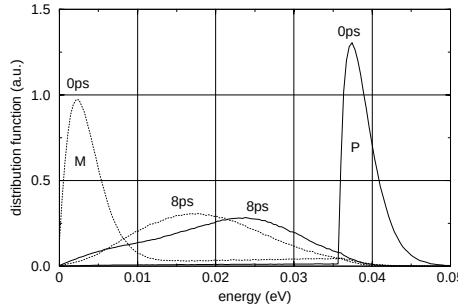


**Fig. 8.** Energy distribution of the $P$ and $M$ ensembles at $t = 0$ and $t = 8$ ps.

(0.036 eV). Above this energy the scattering rate for phonon emission increases rapidly, so that the electrons, penetrating the phonon threshold are intensively scattered back to energies close to zero.

The effect can most conveniently be discussed in the energy domain. The field impulse instantaneously creates a perturbation, represented by ensembles $P$ and $M$ with initial distributions $G^+$ and $G^-$, respectively. Fig. 8 shows the distributions as two peaks, located close to $E = 0$ and above the phonon threshold. The $M$ ensemble is accelerated by the field towards the phonon threshold. The $P$ ensemble is intensively transferred within less than two ps back to low energies and is then accelerated by the electric field.

The peaks in the initial distribution broaden towards the steady state distribution which is reached after about 80 ps in the given example. The $M$ ensemble undergoes an evolution similar to that of the $P$ ensemble, however with same delay, which is responsible for the oscillation in $\langle A \rangle_{\mathrm{im}}(t)$. If the two distributions were equivalent at a certain time, they would oscillate synchronously for later times and no oscillation in the impulse response would show up.

## 5 Monte Carlo Algorithms for Zero Field

The carrier mobility for vanishing field is an important parameter, characterizing the ohmic transport regime. The conventional Monte Carlo method [5] cannot be applied because in the limit $E_s \to 0$ the carrier mean velocity tends to zero while the stochastic velocity component due to thermal excitation keeps its value. Neither can the small signal algorithm presented in the previous section be applied, as the expressions 7 and 8 are singular at $E_s = 0$. This is a consequence of the principle of detailed balance, which makes the scattering term in the Boltzmann equation vanish in thermodynamic equilibrium. However, in that case the stationary distribution function is known to be the Maxwell-Boltzmann distribution, $f_0$, which allows analytical evaluation of 5.

$$G(\mathbf{k}) = \frac{q\mathbf{E}_{\mathrm{im}} \cdot \mathbf{v}(\mathbf{k})}{k_B T_0} f_0(\mathbf{k}) \tag{9}$$

As in the previous section, it is convenient to use the before scattering states of some main trajectory, which have distribution $\lambda f_0 / \langle \lambda \rangle$.

$$G(\mathbf{k}) = \frac{q\mathbf{E}_{\mathrm{im}} \langle \lambda \rangle}{k_B T_0} \cdot \frac{\mathbf{v}(\mathbf{k})}{\lambda(\mathbf{k})} \left\{ \frac{\lambda(\mathbf{k}) f_0(\mathbf{k})}{\langle \lambda \rangle} \right\} \tag{10}$$

This expression gives rise to the following Monte Carlo algorithm.

1) Follow a main trajectory for one free flight and store the before-scattering state $\mathbf{k}$.
2) Compute the weight $w = \frac{\mathbf{v}(\mathbf{k})}{\lambda(\mathbf{k})}$
3) Start a trajectory $\mathbf{K}(t)$ from $\mathbf{k}$ and follow it for time $T$. At equidistant times $t_i$ add $wA(\mathbf{K}(t_i))$ to a histogram $\nu_i$.
4) Continue with the first step until $N$ $\mathbf{k}$-points have been generated.
5) Calculate the time discrete impulse response as $\langle A \rangle_{\mathrm{im}}(t_i) = \frac{q\mathbf{E}_{\mathrm{im}} \langle \lambda \rangle}{k_B T_0} \frac{\nu_i}{N}$.

This algorithm can be specialized to the evaluation of the static zero-field mobility. The latter is given by the long time limit of the velocity step response, which is the time integral of the velocity impulse response. This requires integration of the velocity over a secondary trajectory for a sufficiently long time. However, time integration can be stopped after the first velocity randomizing scattering event has occurred, because in this case the correlation of the trajectory's initial velocity with the after-scattering velocity is lost. Since in thermodynamic equilibrium the before and after-scattering distributions are equal, the secondary trajectories can be mapped onto the main trajectory.

The following algorithm is not restricted to the longitudinal mobility component. Instead, the complete mobility tensor can be evaluated. Note that $\langle \mathrm{v_i} \rangle = \sum_j \mu_{ij} E_j$.

1) Set $\nu = 0$, $w = 0$
2) Follow a main trajectory for one free flight and store the after-scattering state $\mathbf{k}$.

3) Compute a sum of weights: $w = w + \frac{v_j(\mathbf{k})}{\lambda(\mathbf{k})}$
4) Select a free-flight time $t_f = -\frac{\ln(r)}{\lambda(\mathbf{k})}$ and add time integral to estimator:

$$\nu = \nu + w v_i t_f .$$

Alternatively, use the expected value of the time integral: $\nu = \nu + w \frac{v_i}{\lambda(\mathbf{k})}$
5) Perform scattering. If mechanism was isotropic, reset weight: $w = 0$.
6) Continue with the second step until $N$ $\mathbf{k}$-points have been generated.
7) Calculate component of zero-field mobility tensor as $\mu_{ij} = \frac{q\langle\lambda\rangle}{k_B T_0} \frac{\nu}{N}$

Especially the diagonal elements can be calculated very efficiently using this algorithm. Consider a system where only isotropic scattering events take place. Then the product $wv_i$ is always positive, independent of the sign of $v_i$. Therefore, only positive values are added to the estimator, which leads to low variance.

The zero-field mobility of electrons in Si has been calculated as a function of the doping concentration. The frequently used statistical screening model due to Ridley [6][7] overestimates the mobility as shown in Fig. 9. Agreement with experimental data can be achieved by introduction of three fitting parameters [8]. The Monte Carlo algorithm has been used in conjunction with an automatic curve fitting procedure.

## 6 Conclusion

A linearized form of the transient Boltzmann Equation is used to investigate the small signal response of charge carriers in semiconductors. Assuming an impulse-like perturbation in the electric field the linearized equation is split into two common Boltzmann Equations, which are solved by the ensemble Monte Carlo method. In this way the impulse response is understood in terms of the concurrent time evolution of two carrier ensembles. Furthermore, a Monte Carlo algorithm for the calculation of the impulse response for vanishing electric field is given. From this algorithm another one is derived, which is specialized to the calculation of the zero-field mobility.

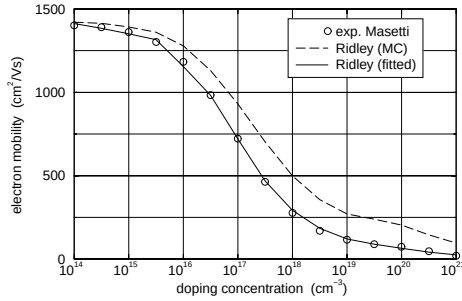


**Fig. 9.** Calibration of the zero-field mobility of electron in silicon.

**Acknowledgment**

This work has been partly supported the European Commission, project NANOTCAD, IST-1999-10828.

## References

1. H. Kosina, M. Nedjalkov, and S. Selberherr. A Monte Carlo method for small signal analysis of the Boltzmann equation, *J.Appl.Phys.*, 87(9), 4308–4314, 2000.
2. M. Nedjalkov, H. Kosina, and S. Selberherr. Monte-Carlo method for direct computation of the small signal kinetic coefficients, in *Simulation of Semiconductor Processes and Devices*, Kyoto, Japan, 155–158, 1999.
3. E. Starikov and P. Shiktorov. New approach to calculation of the differential mobility spectrum of hot carriers: Direct modeling of the gradient of the distribution function by the Monte Carlo method, *Sov. Phys. Semicond.*, 22(1), 45–48, 1988.
4. Y. Pozhela, E. Starikov, and P. Shiktorov. Dynamic NDM at transit time resonance in n-InP, *Semicond.Sci.Technol.*, 7, B386–B389, 1992.
5. C. Jacoboni and P. Lugli. *The Monte Carlo Method for Semiconductor Device Simulation*, Wien-New York, Springer, 1989.
6. B. Ridley. Reconciliation of the Conwell-Weisskopf and Brooks-Herring formulae for Charged-Impurity scattering in semiconductors: Third-Body Interference, *J.Phys.C*, 10, 1589–1593, 1977.
7. T. Van de Roer and F. Widdershoven. Ionized impurity scattering in Monte Carlo calculations, *J.Appl.Phys.*, 59(3), 813–815, 1986.
8. C. Fischer, P. Habaš, O. Heinreichsberger, H. Kosina, P. Lindorfer, P. Pichler, H. Pötzl, C. Sala, A. Schütz, S. Selberherr, M. Stiftinger, and M. Thurner, *MINIMOS 6 User's Guide*. Institut für Mikroelektronik, Technische Universität Wien, Austria, Mar. 1994.